

Physical modelling of YORP-evolved NEA (23187) 2000 PN9 from optical and radar observations

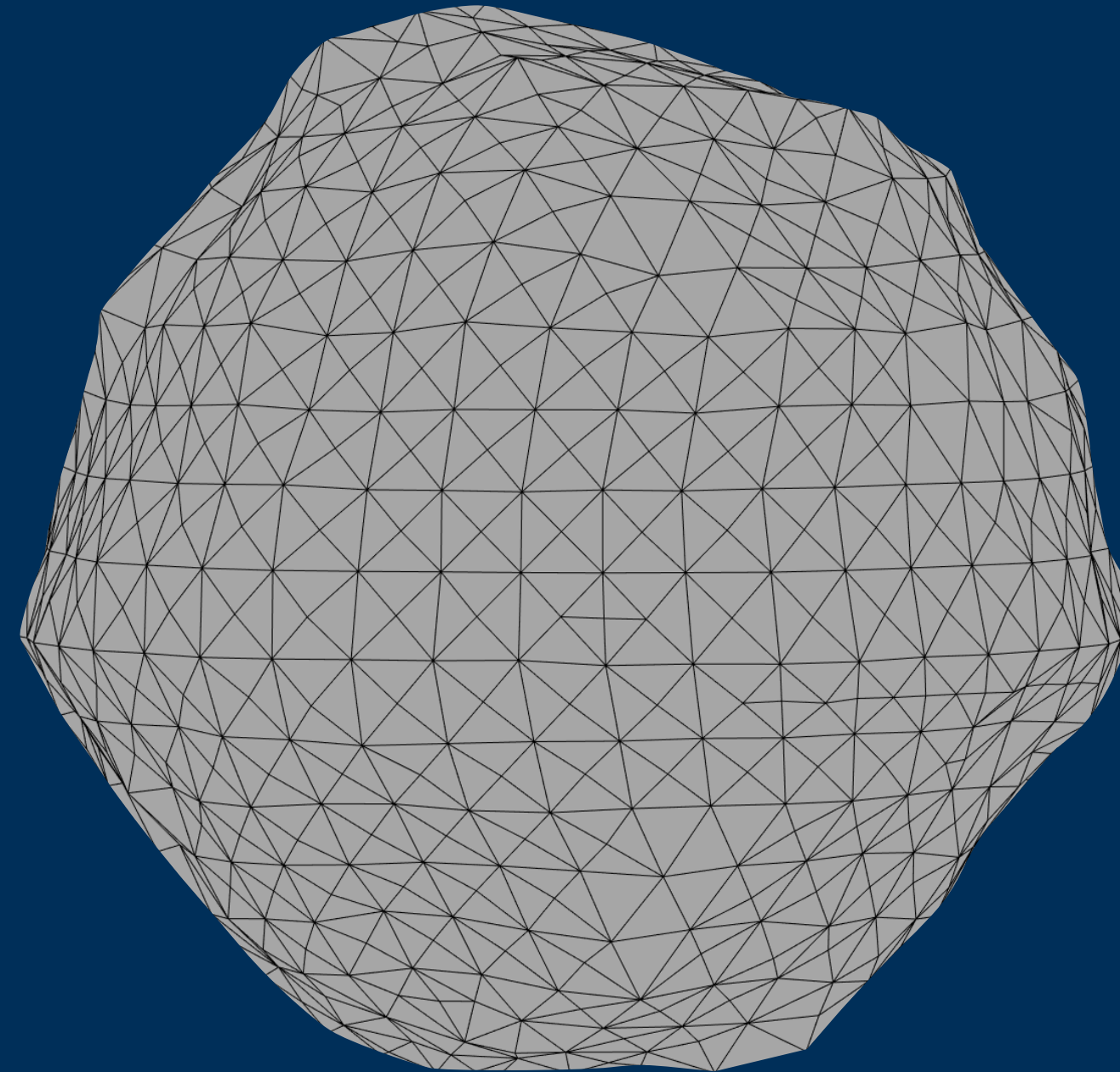
L. Dover (1), S. C. Lowry (1), A. Rožek (2,1), T. Zegmott (1), B. Rozitis (3), S. F. Green (3), C. Snodgrass (2), A. Fitzsimmons (4), P. R. Weissman (5), Y. N. Krugly (6), I. N. Belskaya (6), M. Brozović (7)

(1) University of Kent, UK (lrd27@kent.ac.uk); (2) University of Edinburgh, UK; (3) Open University, UK; (4) Queens University Belfast, UK; (5) Planetary Sciences Institute, USA; (6) V. N. Karazin Kharkiv National University, Ukraine; (7) Jet Propulsion Lab, California Institute of Technology, USA

Abstract

The YORP effect is a thermal torque caused by the absorption and anisotropic re-emission of Solar radiation^[1,2,3]. By inducing changes to spin-state, YORP is the main driver of physical and dynamical evolution of small bodies in the inner Solar System^[4].

We are conducting an optical observing campaign with a sample of near-Earth asteroids. By obtaining rotational lightcurves over multiple apparitions, we are able to detect YORP-induced changes to an asteroid's spin rate.



Further detections of YORP-induced changes in asteroid spin rates will inform and progress models of YORP-driven evolution in the inner Solar System.

For the Apollo-class near-Earth asteroid 2000 PN9, we have combined our optical data with planetary radar observations from the Arecibo and Goldstone observatories. This has allowed us to develop a detailed physical model of the asteroid.

We present our latest analysis of PN9 and report a non-detection of YORP. We do, however, find that the measured shape and spin-state of PN9 indicate that it is a YORP-evolved body.



Observational Data

Rotation Period

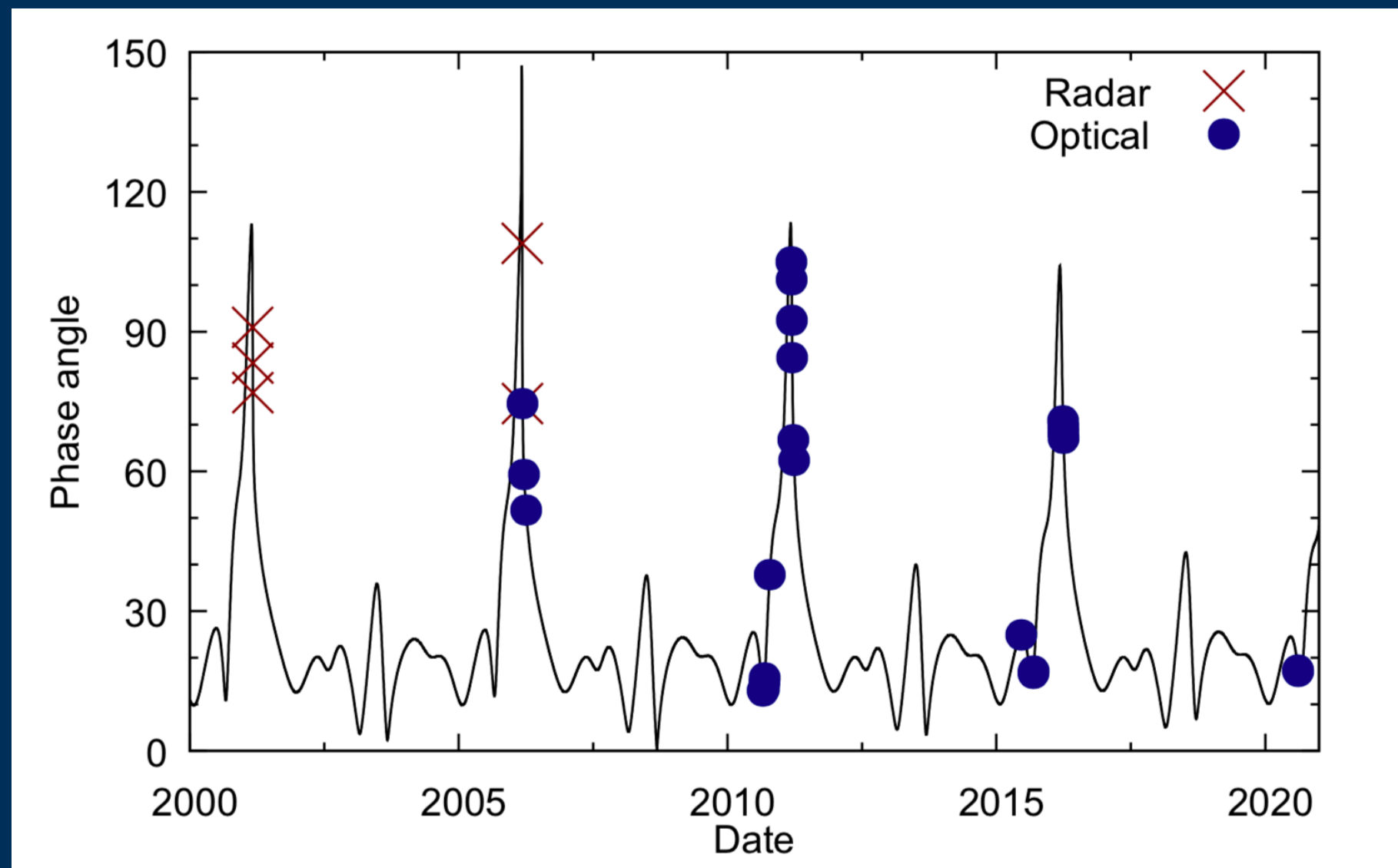


Fig. 1: Solar phase angle of PN9 from 2000 to 2020, with radar (red cross) and optical (blue circle) observations marked.

- 29 optical lightcurves* between March 2001 and March 2016**
- Radar observations with Arecibo (2001) and Goldstone (2001, 2006). Both continuous wave spectra and delay-Doppler imaging were obtained in 2001 and 2006
- [Click here to view a list of all observations](#)

*Some 2006 and 2016 dates have multiple lightcurves each night

**Further observations completed in Aug 2020, analysis in progress

- Convex inversion^[5,6] methods were applied to the optical lightcurves to optimise the convex shape and period of PN9
- A sidereal period of 2.5329 ± 0.0002 hr was measured, which is similar to earlier synodic periods^[7,8]
- This lightcurve-derived period was used as the input for radar modelling to reduce computation time

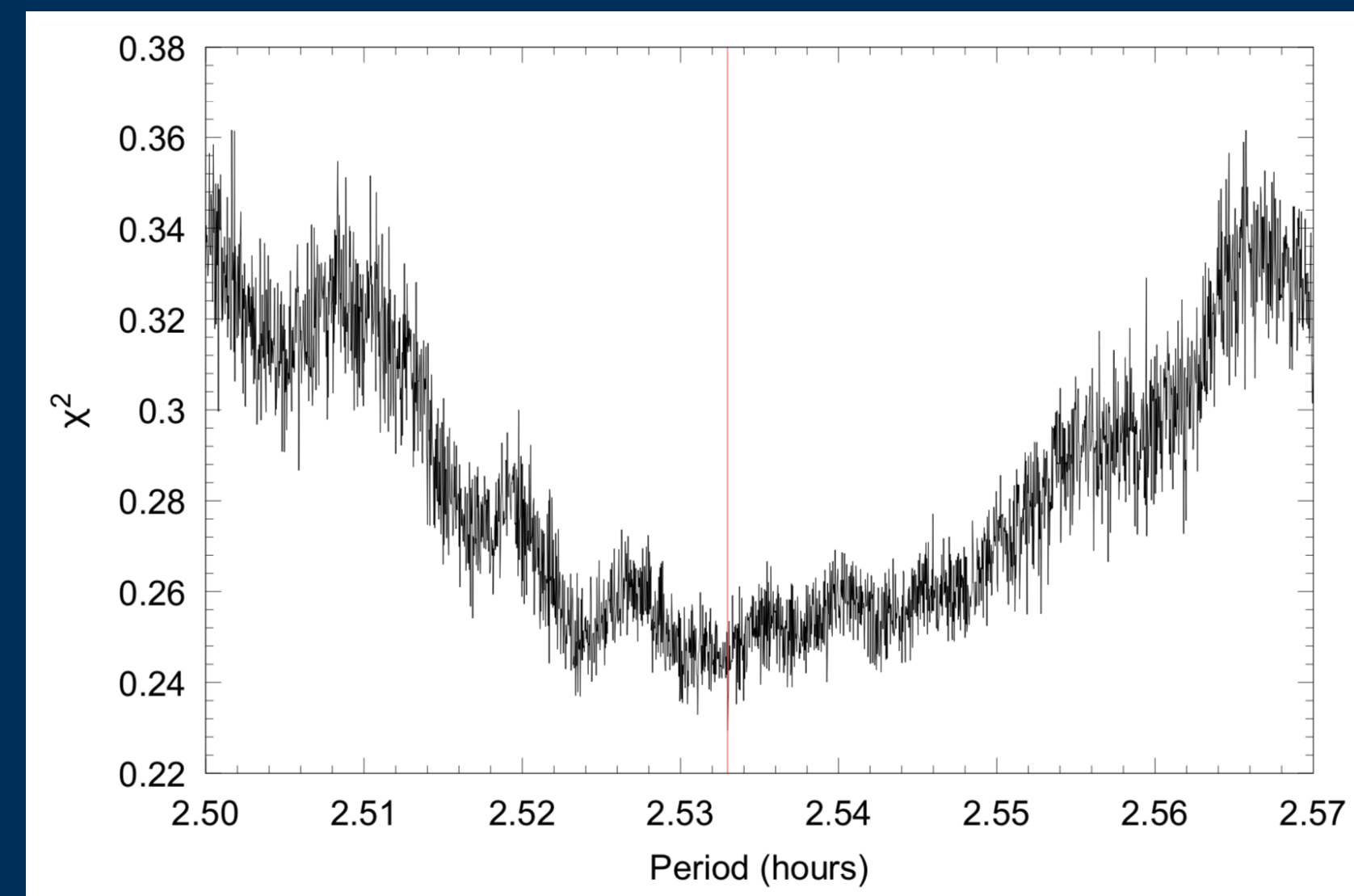


Fig. 2: The results of a period scan using lightcurves. The period with the χ^2 best fit is marked with a vertical red line.

Developing a Physical Model

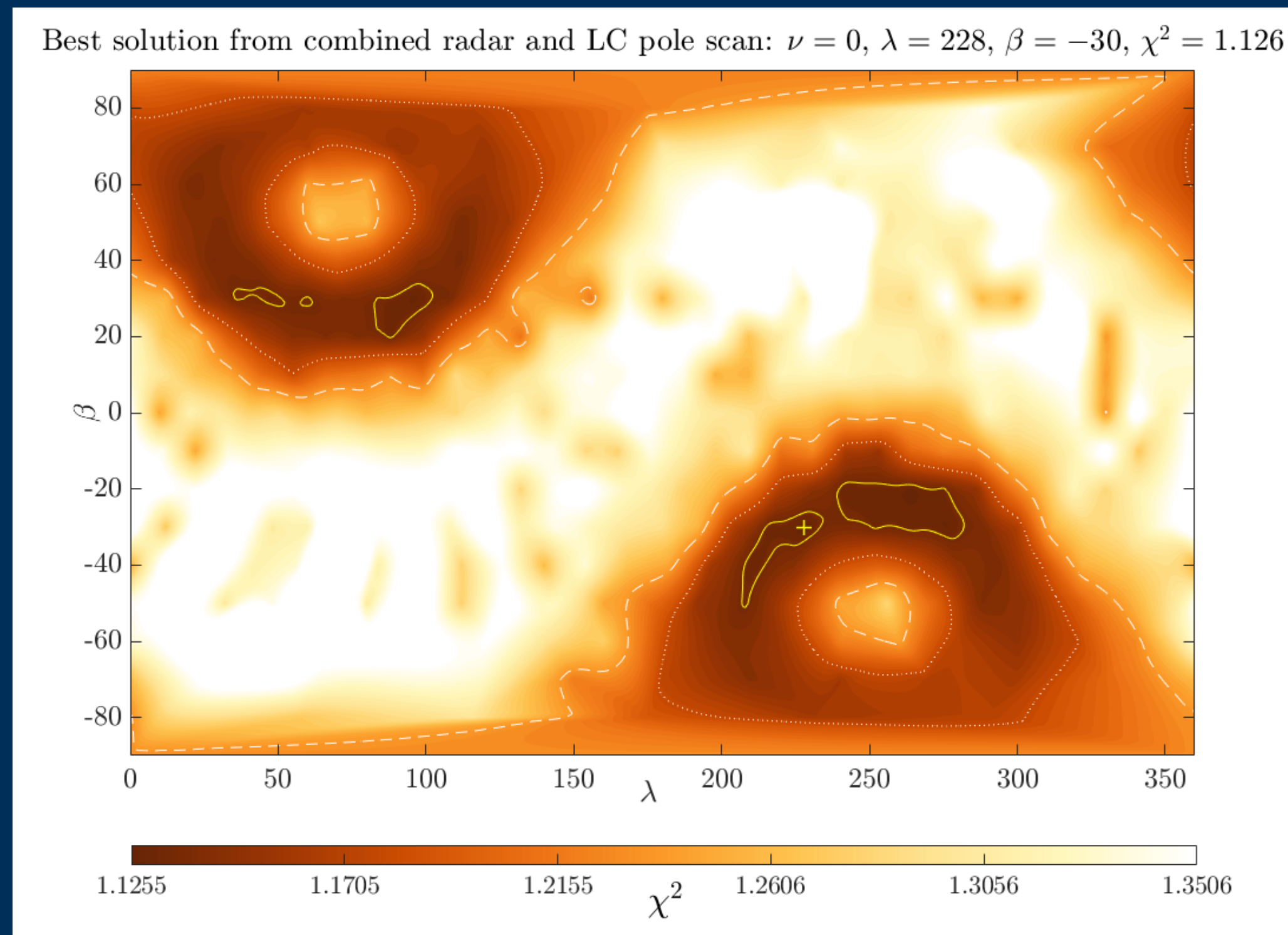


Fig. 3: The results of a pole-scan using radar and lightcurves. For each pole solution in ecliptic coordinates λ and β , the χ^2 fit of the solution is plotted for a colour range where the global minimum χ^2 is black and the maximum is white. The best solution is marked with a yellow '+'. The dotted and dashed white lines enclose regions where χ^2 is within 1% and 5% of the best solution respectively.

To determine the the orientation of PN9's rotational axis, we set up a $10^\circ \times 10^\circ$ grid of poles covering the celestial sphere. For each pole, the SHAPE software package^[9] was used to optimise the model's shape and period to fit the lightcurves, continuous wave spectra and delay-Doppler imaging.

Penalties were applied in SHAPE to discourage non-physical features such as extreme concavity, surface spikes, and significant centre of mass deviation. The model assumes principal axis rotation and zero YORP acceleration.

Fig. 3 shows the χ^2 fit for each pole solution with the best fitting model marked at $\lambda=228^\circ$ $\beta=-30^\circ$. However, χ^2 converges to two opposite regions; this pole degeneracy indicates that SHAPE cannot determine if PN9 is a prograde or retrograde rotator. The model for the best-fitting northern pole solution lies directly opposite the global χ^2 minimum, with an identical period and very similar shape.

The physical model at the global χ^2 minimum is presented in this poster, however a northern pole solution has not yet been discounted.

Radar Fits

The model of PN9 can be used to generate artificial delay-Doppler images and continuous wave spectra. We generated synthetic data to match each radar observation to enable direct comparison.

As shown in Figs. 4 & 5, the model of PN9 accurately reproduces the radar observations, verifying the accuracy of the model.

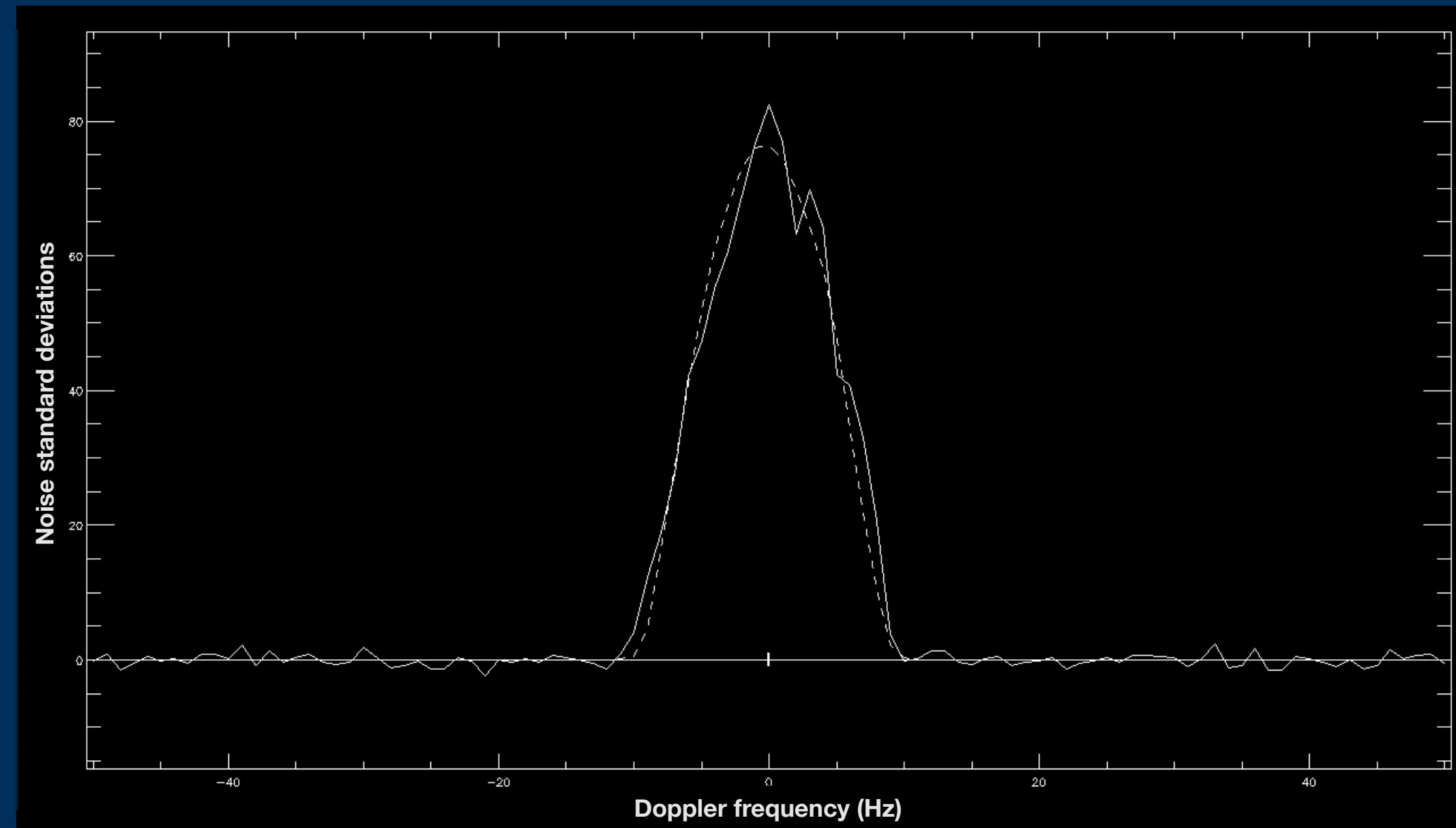


Fig. 4: Comparison of the model continuous-wave spectra (dashed) with the observed spectra (solid) from Arecibo on 2001-03-04. [Click on the image to see the full 2001 Arecibo continuous wave dataset](#) (opens webpage).

Click on these panels to view animation!
(opens webpage)

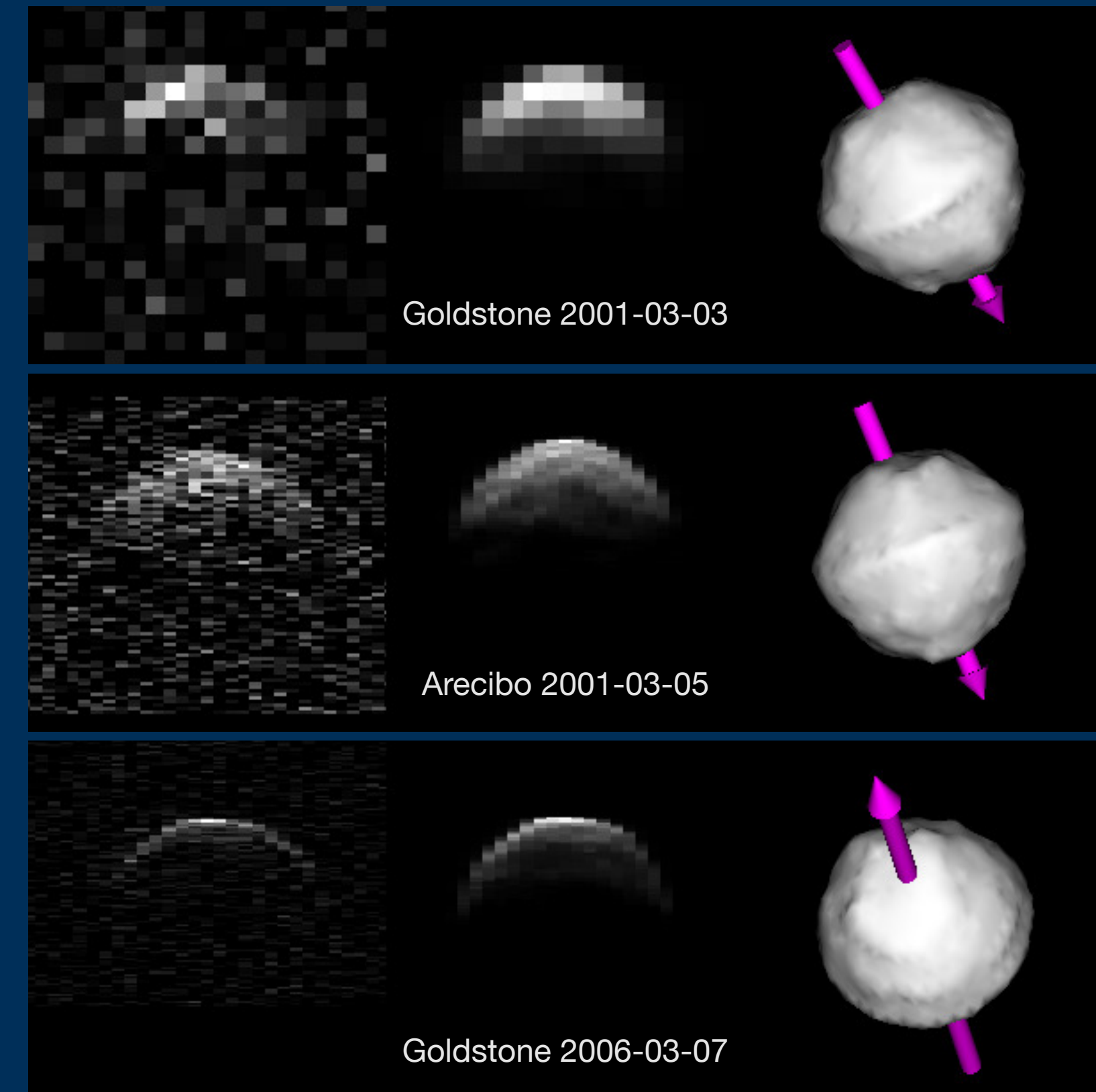


Fig. 5: Comparison of delay-Doppler images (left) with a synthetic delay-Doppler image (centre) generated using the best fit physical model. The plane-of-sky view for the physical model at the time of observation is shown on the right. [Click on each panel to view the full datasets showing the asteroid's rotation](#) (opens webpage).

Physical Characteristics

PN9 is rotating close to the spin-breakup limit and has a distinctive ‘top-shaped’ geometry with a prominent equatorial bulge. This shape can be the result of YORP-spin up^[10], indicating that PN9 is a YORP-evolved asteroid.

As a relatively large and symmetrical asteroid, PN9 is unlikely to be currently experiencing strong YORP acceleration. The highly symmetrical shape also produces low amplitude lightcurves, making it difficult to measure changes to the asteroid’s period. As such, our ongoing analysis has not yet shown YORP acceleration for PN9.

Parameter	Value
Rotation Period	2.532972 ± 0.000015 hr
Rotational pole orientation (Ecliptic coordinates)	$\lambda = 228^\circ, \beta = -30^\circ$
Max extent (x,y,z)	1.885 km x 1.888 km x 1.780 km
DEEVE (2a, 2b, 2c) (Dynamically equivalent equal-volume ellipsoid)	1.791 x 1.770 x 1.710 km
Surface area	9.993 km ²
Volume	2.840 km ³
Model vertices	1000
Model facets	1996

Table 1: Parameters of the physical model

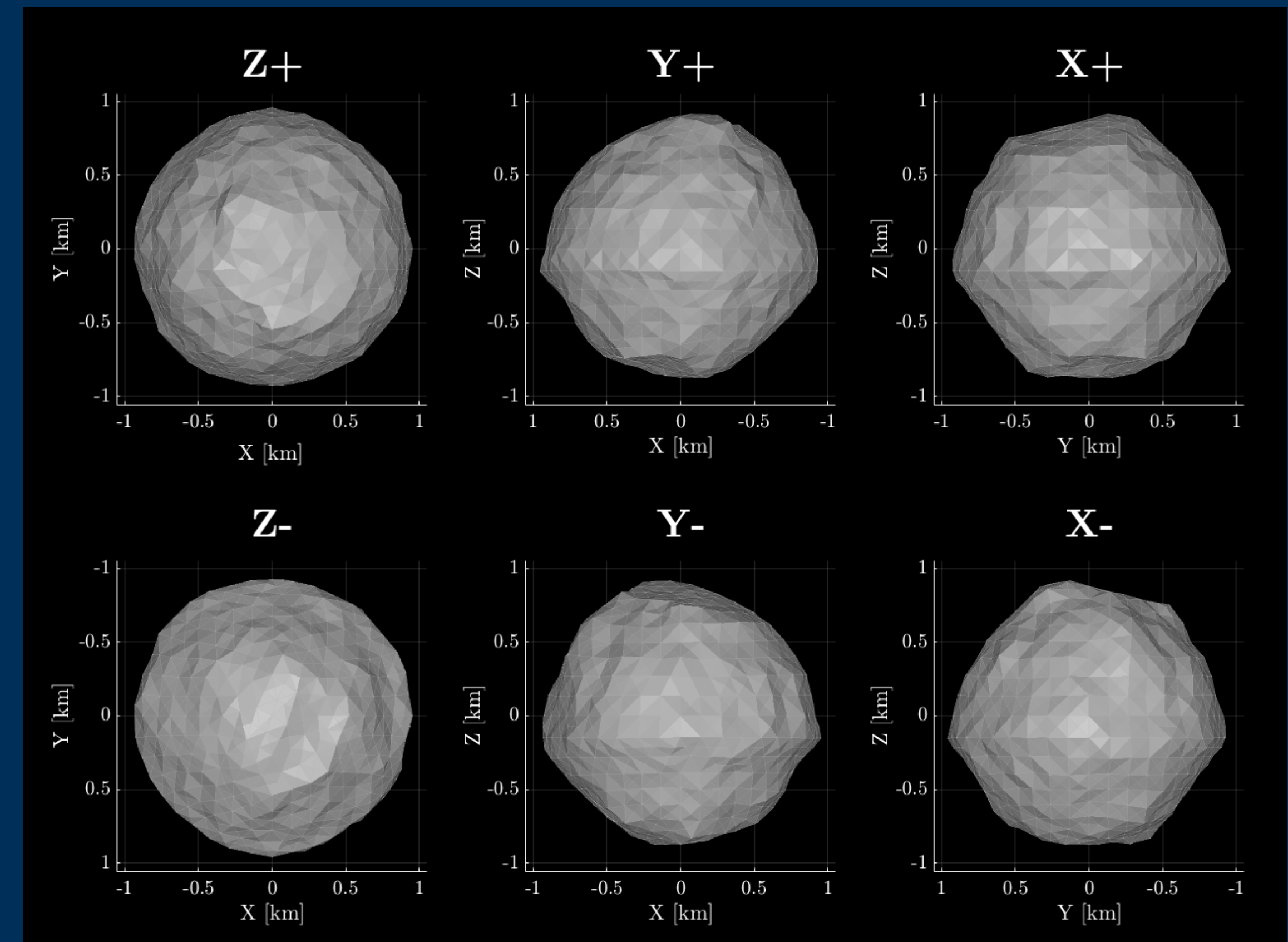


Fig. 6: The best-fit model from SHAPE constructed from combined radar and optical data. This model assumes zero YORP acceleration and principal axis rotation. The top row shows the model from the positive end of the Z, Y and X axes. The bottom row shows the model from negative end of the Z, Y and X axes. The Z-axis is aligned with the rotational pole, which is the shortest axis of inertia. The X-axis is arbitrarily set such that it viewed from the positive end for the plane-of-sky during the first radar observation in 2001.

Conclusions

- We have developed a detailed physical model of 2000 PN9 using optical lightcurves and radar continuous-wave spectra and imaging.
- The short rotation period, symmetrical shape and equatorial ridge are indicative of past YORP spin-up, thus PN9 is a YORP-evolved body.
- We find PN9 to be the largest known asteroid to have a ‘classical’ top-shaped geometry, with a mean diameter of 1.85 ± 0.14 km.
- Our measured rotation period of 2.532972 ± 0.000015 hr places PN9 as the fastest-rotating ‘YORPoid’ that is not part of a multiple system.
- PN9 is rotating close to the spin-breakup limit, and future work may reveal evidence of mass-lofting.

Future Work

- Update the physical model and YORP analysis using recent lightcurves from the 2.6m Shajn telescope and 2.5m Isaac Newton Telescope in August 2020 (*in progress*).
- Conduct a thermal analysis with Spitzer thermal-IR lightcurves taken on 11 November 2015. This will enable a prediction of YORP strength and constrain albedo and surface roughness, with the potential to detect dust lifting off the surface (*near future*).
- We will use our detailed physical model to map gravitational slopes across the asteroid and perform a structural analysis to determine surface cohesion properties^[11] (*near future*).
- Continue optical observations to search for changes in period due to YORP acceleration or mass-lofting events (*long term*).

Acknowledgements

The authors would like to thank R. Ya. Inasaridze, V. A. Ayvazian, V. V. Romyantsev, V. G. Chiorny, I. V. Reva, M. A. Krugov, I. E. Molotov, M. W. Busch, M. C. Nolan, A. A. Hine, V. Negrón, L. A. M. Benner and M. D. Hicks for their contributions to this work. LD, SCL and TZ would like to thank the UK Science and Technology Facilities Council for their support.

References

- | | |
|--|---|
| [1] Rubincam, D. P. (2000). <i>Icarus</i> 148,2. | [7] Belskaya, I. N. et al. (2009). <i>Icarus</i> 201, 167. |
| [2] Lowry, S. C. et al. (2007). <i>Science</i> 316, 272. | [8] Warner, B. D. (2016). <i>Minor Planet Bulletin</i> 43, 240. |
| [3] Taylor, P et al. (2007). <i>Science</i> , 316, 274 | [9] Magri, C. et al. (2007). <i>Icarus</i> , 186, 152 |
| [4] Bottke, W. F. et al. (2006). <i>AREPS</i> 34. | [10] Walsh, K. J. et al. (2008). <i>Nature</i> 454, 188. |
| [5] Kaasalainen, M. & Torppa, J. (2001). <i>Icarus</i> , 153, 24 | [11] Rozitis, B. et al. (2014). <i>Nature</i> 512, 174 |
| [6] Kaasalainen, M. et al. (2001). <i>Icarus</i> , 153, 37 | |



This poster participates in the

OSPA

Outstanding Student Poster
Award Contest
